Abstract

A multi-year research programme is underway to develop and deliver spectral-based digital cameras for imaging cultural heritage at the National Gallery of Art, Washington DC, and the Museum of Modern Art, New York. The cameras will be used for documentation, production imaging, and conservation science. Three approaches have undergone testing: a liquid-crystal tunable filter (LCTF) coupled with a monochrome camera, a six-position filter wheel containing absorption filters coupled with a monochrome camera, and a two-position filter slider containing absorption filters coupled with a colour-filter array (CFA) colour camera. The last approach is the most practical as it uses conventional digital photography methodologies and equipment and can easily be incorporated into existing museum workflows. A virtual camera model was created that predicted camera signals from incident radiation and was used to design a pair of absorption filters. The filters were fabricated and tested using a commercial CFA digital camera. Our first experiments have been very promising: Average accuracy was under 1 CIEDE2000 and about 1.5 per cent RMS for both calibration and verification data. This level of performance was superior to our other, more complex approaches.

Keywords

spectral imaging, digital photography, colour management, cultural heritage digital archiving

Spectral imaging using a commercial colour-filter array digital camera

Roy S Berns, Lawrence A Taplin, Mahdi Nezamabadi, Mahnaz Mohammadi and Yonghui Zhao
Munsell Color Science Laboratory
Chester F Carlson Center for Imaging Science
Rochester Institute of Technology
54 Lomb Memorial Drive
Rochester
NY 14623, USA
E-mail: berns@cis.rit.edu
Web site: http://art-si.org/

Introduction

Imaging is an important technique in the scientific examination of art. Its main use has been for visual documentation. Photographs have long been used to document condition before and after transit, microscopic examinations, conservation treatments, and so on. They are used to enable colour reproductions in books and through the Internet. Images using materials with spectral sensitivities in non-visible regions of the electromagnetic spectrum such as infrared and X-ray are equally important to the visible spectrum. Although images are used to record scientific examinations, they are used infrequently as an analytical tool. That is, the amount of colourant in a photographic material would be used to relate to physical properties of the art. In contrast, astronomy, remote sensing, and medicine have exploited this capability for many years. The advent of digital imaging offers increased opportunities to exploit images for the scientific examination of art.

A research programme is underway at Rochester Institute of Technology to develop an image acquisition system that records reflection information as a function of wavelength (Berns et al. 2004b, 2004c, Imai 1998, Imai et al. 2000a, 2000b, 2002). Three techniques have been evaluated. The first combines a monochrome area-array camera with a liquid-crystal tunable filter, resulting in a 31-channel imaging spectrometer. The second technique combines the same type of camera with a filter wheel containing six absorption filters; using appropriate colour targets and mathematical transformations, spectral images are estimated from the six channels. The third technique uses a colour-filter array camera and a pair of absorption filters, also yielding six channels; the same approach is used to estimate spectral data as the six-position filter wheel. This last technique holds great promise because commercial professional-quality digital cameras can be used. This method was tested using a Sinarback 54H.

Equipment

A Sinarback 54H digital cameraback coupled with a Sinar M shutter, P3 body, and 105 mm HR lens were used in this experiment. Sinar CaptureShop 4.1 controlled its operation. This camera incorporates a Kodak KAF-22000CE sensor with a resolution of 5440 pixels × 4080 pixels. The 'four-shot' mode was used resulting in 5440 × 4080 non-interpolated RGB data. The cameraback was modified by replacing its infrared cover glass with clear glass. The nominal spectral sensitivities of the sensor are plotted in Figure 1. A pair of Broncolor F1200 HMI lights were used. They produced a correlated colour temperature of 4966 K and an illuminance of 9300 lux at the object plane.

Seven targets were evaluated: the GretagMacbeth ColorChecker DC, the GretagMacbeth ColorChecker, the ESSER TE221 scanner target, a custom target of Gamblin conservation colours, an acrylic-medium blue target with a number of different blue pigments, and two small oil paintings. They were used in different combinations as calibration and verification data. For the virtual camera model, a Macbeth XTH integrating sphere spectrophotometer was used (380–750 nm); for the imaging experiments, a Macbeth SpectroEye spectrophotometer was used (380–730 nm) to measure the spectral reflectance factor of each target.

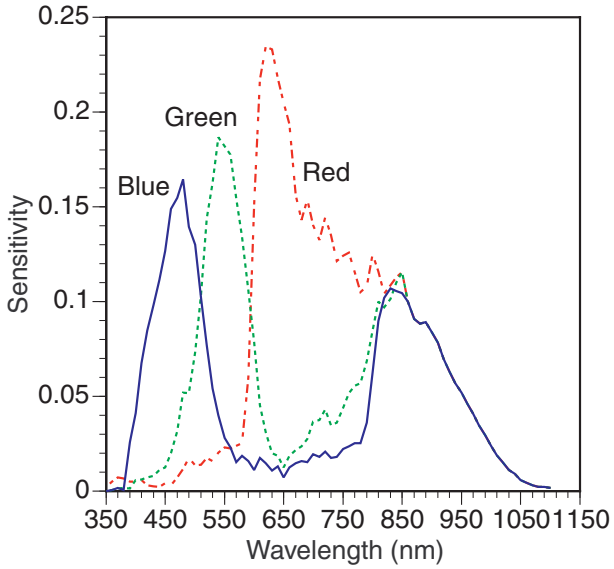

Figure 1. Spectral sensitivities of the Kodak KAF-22000CE colour-filter array sensor

Virtual camera model

A virtual camera model was created to select sets of glass filters, shown by Equation (1):

$$S_{\lambda,i} = F_\lambda I_\lambda C_{\lambda,i} \tag{1}$$

where λ is wavelength, ranging from 380–750 nm at 10 nm intervals, $C_{\lambda,i}$ is the spectral sensitivity of the camera for the ith channel at each wavelength, I_λ and F_λ are spectral transmittances of infrared (IR) cut-off and glass filters, respectively, and $S_{\lambda,i}$ is the resulting spectral sensitivity for the entire camera system. For an object with reflectance factor, R_λ, a camera signal, D_i, is calculated by Equation (2):

$$D_i = \sum_{\lambda=380}^{750} (R_\lambda L_\lambda S_{\lambda,i}) + n_i \tag{2}$$

where L_λ is the relative spectral power distribution of the illuminant, and n_i is a noise term.

Spectral reflectance is estimated from camera signals by a matrix transformation:

$$\hat{\mathbf{R}} = \mathbf{M}_s\mathbf{D} \tag{3}$$

where $\hat{\mathbf{R}}$ is the $(\lambda \times 1)$ vector of estimated reflectances, $\mathbf{D}$ is a $(i \times 1)$ digital count vector, and $\mathbf{M}_s$ is the $(\lambda \times i)$ transformation matrix (subscript s represents spectral). The transformation matrix was derived using 2500 virtual pixels and the measured spectral reflectance for each sample of a calibration target; a generalized pseudo inverse calculation incorporating singular value decomposition was used to calculate the matrix. Finally, tristimulus values, $\mathbf{T}$, a (3×1) vector, are calculated from estimated spectra:

$$\mathbf{T}_s = \mathbf{A}'\hat{\mathbf{R}} \tag{4}$$

where $\mathbf{A}$ is a $(\lambda \times 3)$ matrix of ASTM tri-stimulus weights.

The Schott filter glass catalogue was used to create a set of possible filters. Filters could be single pieces of glass at 1–4 mm thickness or 'sandwiches' of 1 and 3 mm or 2 and 2 mm. Beer's Law and the Fresnel equations were used to create these sandwiches. There were 2830 theoretical filters. Because the camera system would use two filters sequentially, the number of filter pair combinations became 2,831,010. Based on initial noise-free calculations, throughput considerations, and spectral accuracy, the number of candidate combinations was reduced to 30,000.

Using the Esser target as the calibration target, all 30,000 filter sets were tested. That is, Equations (1) and (2) were used to create a six-channel digital image. The image and measured spectral reflectance data were used to derive a transformation matrix. Finally Equation (3) was used to estimate spectral reflectance for the calibration and verification targets. For example, the relationship between spectral and colourimetric accuracy is plotted in Figure 2.

Twenty-five filter pairs were selected based on their spectral and colourimetric accuracy and spectral transmittance. These were analysed in detail. One pair was selected for fabrication and experimentation.

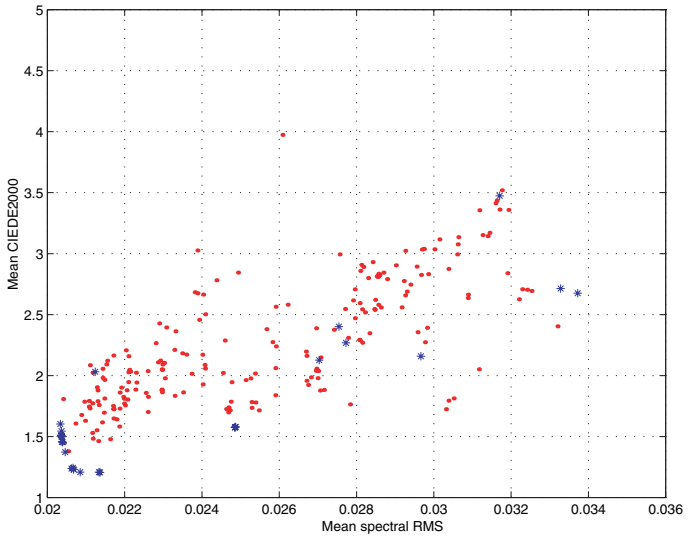

Figure 2. Mean colour differences (ΔE_{00} for D65) compared with mean spectral error, RMS, in the estimation of the Esser calibration target for the selected 30,000 filter pairs. Blue asterisks mark 25 filter pairs selected for further analysis

Experimental

The spectral sensitivities and the opto-electronic conversion function (OECF) of the camera were measured according to ISO standards, 14524 (1999) and 17321 (2003). The normalized spectral sensitivities of the modified Sinar 54 are plotted in Figure 3. These filters are sampling the visible spectrum unevenly; three of the filters have their peaks in wavelength locations well suited for colourimetric imaging, 450 nm, 550 nm, and 600 nm. A metric for colourimetric accuracy, μ-factor (Vora et al. 1993), was calculated for both the six-channel and 'production' three-channel camera for several combinations of taking and rendering illuminants shown in Table 1. A μ-factor of unity corresponds to perfect colour accuracy, only achievable when the camera's spectral sensitivities are linearly

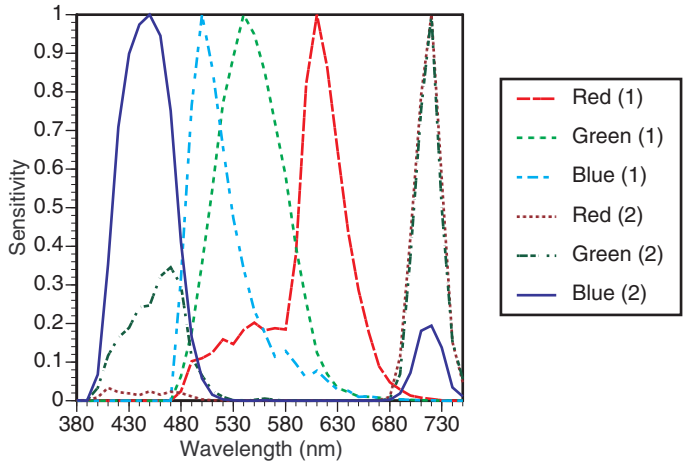

Figure 3. Normalized (by peak height) spectral sensitivities of the modified Sinar 54H

related to CIE colour-matching functions and the taking and rendering illuminants are identical. For high-accuracy colour imaging, we seek cameras with μ-factor above 0.9 for matched taking and rendering illuminants. The production camera was made by using a single blue-green absorption filter with very similar spectral properties to that of the removed cover glass. For the production camera, μ-factor ranged between 0.68 and 0.85; these values are typical for CFA cameras. The modified camera resulted in higher potential colour accuracy; μ-factor increased in all tested cases. An interesting result was that the six-channel camera had higher values than a theoretical colourimetric camera when taking and rendering illuminants were unmatched. Increasing the number of channels improved the colourimetric robustness. These calculations also indicate the importance of illumination spectral power distribution on colour accuracy.

Images were taken of a uniform grey background, the ColorChecker DC (the calibration target), and the ColorChecker (the verification target) using both the modified and production camera. All the images were digitally flat fielded using the grey background. Three one-dimensional look-up tables were derived that converted encoded digital data to linear photometric data based on the measured OECF. Using the same technique described for the virtual camera, a transformation was derived for the modified camera that estimated spectral reflectance from the post-LUT camera signals.

For both systems, a further colourimetric transformation was derived that consisted of a matrix converting camera signals to tristimulus values, **T**, and a second photometric correction, **Q**, commonly used to characterize CRT displays (Berns 2000C):

$$\mathbf{T}_c = \mathbf{M}_c\mathbf{Q} \tag{5}$$

$$\mathbf{Q}_i = [k_{g,i}(D_i/D_{max}) + k_{o,i}]^{\gamma_i}. \tag{6}$$

Differences in surface characteristics between the OECF and colour-calibration targets necessitated the second photometric correction. Nonlinear optimization was used to derive $\mathbf{M}_c$ and the $k_{g,i}$, $k_{o,i}$, and γ_i coefficients where the objective function was minimizing both the average and maximum CIEDE2000 for the calibration target. For the modified camera, $\mathbf{M}_c$ was a (3 × 6) matrix; for the production camera, $\mathbf{M}_c$ was a (3 × 3) matrix.

For the modified camera, Equation (5) often results in greater colour accuracy than Equation (4) owing to the nonlinear optimization. Using parameric decomposition (Fairman 1997), the estimated spectra were adjusted to achieve the same tri-stimulus values as obtained using nonlinear optimization:

$$\hat{\mathbf{R}}_c = \mathbf{A}(\mathbf{A}'\mathbf{A})^{-1}\mathbf{T}_c + (\mathbf{I} - \mathbf{A}(\mathbf{A}'\mathbf{A})^{-1}\mathbf{A}')\hat{\mathbf{R}} \tag{7}$$

where **I** is an identity matrix.

Results and discussion

The imaging performance for both the calibration and verification targets is compiled in Tables 2–4. The average colourimetric performance for the production Sinar was quite reasonable for a colour managed digital camera (Table 2). The nonlinear optimization technique was an effective technique to profile the camera. However, the maximum errors were large. The inherent limitations of the sensor's spectral sensitivities limited performance, consistent with the data shown in Table 1.

The modified six-channel Sinar was used to estimate spectral reflectance based on Equation (4), the performance listed in Table 3. Average spectral fit was 1.6 per cent RMS over the spectral range of 380–730 nm. Given the inherent constraints of the CFA's spectral sensitivities and the extent of modification by a pair of coloured filters, these results were very good. The colourimetric accuracy was similarly high. However, for the calibration data, the maximum colourimetric error was large. Optimizing average spectral accuracy does not lead to optimal colourimetric performance.

Table 1. μ-factor values for each listed combination of taking and rendering illuminants for a production Sinar 54H, the six-channel modified Sinar, and a theoretical camera with spectral sensitivities equal to colour-matching functions

Taking/rendering illuminant	Production Sinar	Modified 6-channel Sinar	Theoretical Colourimetric
Tungsten/D65	0.75	0.95	0.96
HMI/D65	0.68	0.73	0.53
D65/D65	0.85	0.96	1.00

Table 2. Performance metrics comparing a conventional small-aperture in situ spectrophotometry with the 'production' Sinarback 54H colourimetric image for the calibration (ColorChecker DC) and verification data (ColorChecker) using Equation (5)

ΔE_{00}	ColorChecker DC	ColorChecker
Mean	1.9	2.6
Maximum	10.9	9.2
Standard deviation	1.9	2.0

Table 3. Performance metrics comparing a conventional small-aperture in situ spectrophotometry with the modified Sinarback 54H spectral image for the calibration (ColorChecker DC) and verification data (ColorChecker) using Equation (4). The metameric index incorporates a parameric correction (Fairman 1997) that corrects the test spectrum to a perfect colourimetric match for either illuminant D65 or A followed by a colour difference assessment under either illuminant A or D65, respectively

	ΔE_{00} (D65, 2°)	RMS (%)	Metameric index (D65 $\rightarrow$ A, ΔE_{00})	Metameric index (A $\rightarrow$ D65, ΔE_{00})
		ColorChecker DC		
Average	1.4	1.6	0.5	0.6
Maximum	13.3	4.0	5.0	6.5
Standard deviation	1.6	0.6	0.8	0.9
		ColorChecker		
Average	1.2	1.6	0.3	0.4
Maximum	3.5	2.6	1.4	1.7
Standard deviation	0.9	0.6	0.4	0.4

Table 4. Performance metrics comparing a conventional small-aperture in situ spectrophotometry with the modified Sinarback 54H spectral image for the calibration (ColorChecker DC) and verification data (ColorChecker) using Equations (4) and (5)

	ΔE_{00} (D65, 2°)	RMS (%)	Metameric index (D65 $\rightarrow$ A, ΔE_{00})	Metameric index (A $\rightarrow$ D65, ΔE_{00})
		ColorChecker DC		
Average	0.9	1.5	0.5	0.6
Maximum	3.0	3.9	5.0	5.9
Standard deviation	0.7	0.6	0.8	0.8
		ColorChecker		
Average	0.9	1.6	0.3	0.4
Maximum	2.2	2.6	1.4	1.5
Standard deviation	0.5	0.6	0.4	0.4

Combining the spectral and colourimetric transformations, Equation (6), resulted in excellent performance, as shown in Table 4. Both average and maximum errors are small. The spectral fits for the ColorChecker are plotted in Figure 4. As a comparison, we have used a monochrome sensor coupled with a liquid-crystal tunable filter to capture 31-band images (Berns et al. 2004c). The average performance for the ColorChecker was 1.5 ΔE_{00} and 1.4 per cent RMS (over the spectral range of 400–700 nm). Liang et al. (2004) tested a 13-channel system using a monochrome sensor and interference filters; the average results for the ColorChecker was 1.2 ΔE_{00} and 1.4 per cent RMS (over the spectral range of 400–700 nm) using interpolation to transform the multi-channel signals to

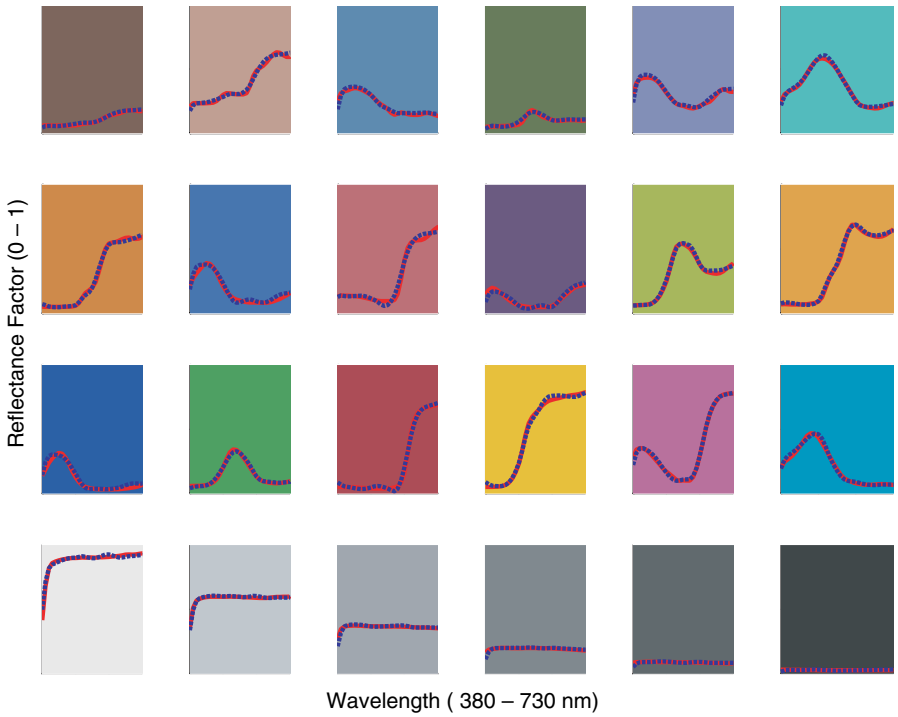

Figure 4. Spectral estimation accuracy of the six-channel modified Sinar 54H (dashed blue line) compared with in situ spectrophotometry (solid red line) of the GretagMacbeth ColorChecker (coloured backgrounds are approximate)

spectral reflectance. The modified Sinar was able to achieve equivalent performance compared with considerably more complex technologies.

As a final analysis, the transformation vectors from camera signals to spectral reflectance, $\mathbf{M}_s$, are plotted in Figure 5. The absolute scalar magnitude indicates which filter has the dominant influence on estimating spectral reflectance at a given wavelength. The goal is to have an appreciable signal for at least one channel at every wavelength. With the exception of 380, 390, and 680 nm, this goal was achieved. By definition, these vectors are affected by the spectral properties of the calibration target. It should be possible to improve these wavelengths by a more optimal calibration target, a current research topic (Mohammadi et al. 2004).

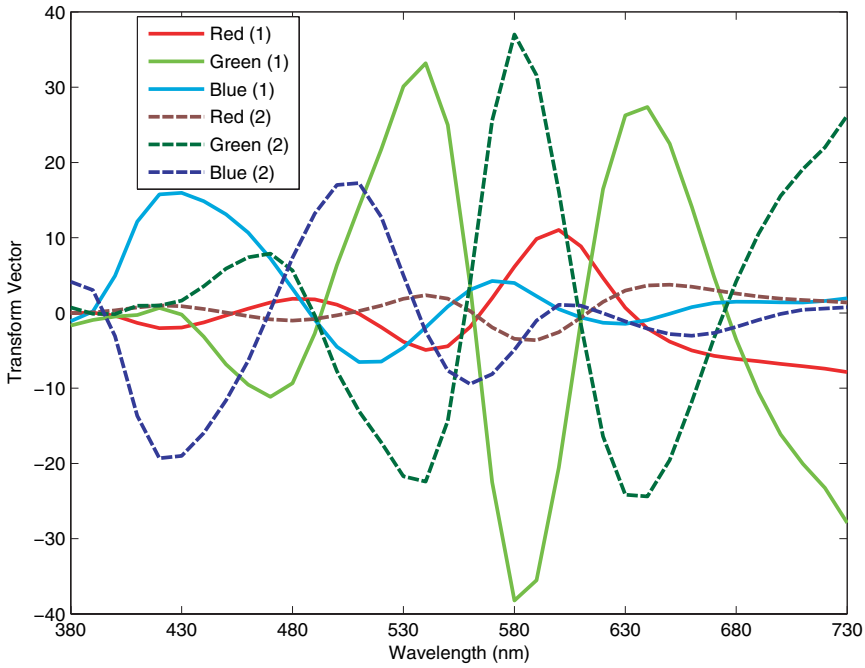

Figure 5. Transform vectors from camera signals to spectral reflectance, M_s

Conclusions

A high-resolution, medium format, production colour-filter-array (CFA) digital cameraback, the Sinar 54H, was modified to facilitate spectral imaging. Modifications included replacing the IR filter with clear glass and fabricating a pair of filters that when positioned sequentially, resulted in six channels sampling the visible spectrum between about 390 and 760 nm. Transformations were derived enabling both spectral estimation and high-accuracy colourimetric imaging. The accuracy achieved equaled or exceeded much more complex imaging systems.

This approach offers numerous advantages. This type of camera is very familiar to museum-imaging professionals. Thus, spectral-based imaging can be readily incorporated into the museum imaging workflow, greatly improving efficiency by eliminating visual editing. Scientific imaging can be the providence of the imaging department rather than requiring the resources of a conservation scientist with colour imaging expertise. Since only two images are captured, image registration is straightforward, often a limiting factor in achieving efficiency, for example Liang et al. (2004) and Ribés et al. (2004). If commercialized, the multi-filter CFA camera can produce both colour-managed RGB and spectral digital masters. The RGB images can be used to create derivative images for web-based display and for on-demand and catalogue printing. The spectral image can be used for conservation science, lighting design by rendering the image under various lighting conditions (Berns and Merrill 2002), and future pedantic research. In conservation, the spectral image can be used as an aid in inpainting (Berns et al. 2002, Berns and Imai 2002) and pigment identification (Liang et al. 2004), for documenting long-term colour changes (Saunders and Cupitt 1993), digital rejuvenation (Berns 2004, Berns et al. 2004a), and pigment mapping (Baronti et al. 1998), among others.

Acknowledgements

This research was supported by the Andrew W Mellon Foundation, the National Gallery of Art, Washington DC, the Museum of Modern Art, New York, and Rochester Institute of Technology.

References

Baronti, S, Casini, A, Lotti, A, and Porcinai, S, 1998, 'Multispectral imaging system for the mapping of pigments in works of art by use of principal-component analysis', *Applied Optics* 37, 1299–1309.

Berns, R S, Krueger, J and Swicklik, M, 2002, 'Multiple pigment selection for inpainting using visible reflectance spectrophotometry', *Studies in Conservation* 47, 46–61.

Berns, R S and Imai, F H, 2002, 'The use of multi-channel visibile spectrum imaging for pigment identification' in *Preprints of the 13th Triennial Meeting of the ICOM Committee for Conservation, ICOM, Rio de Janeiro*, 217–222.

Berns, R S and Katoh, N, 2002, 'Methods for characterizing displays' in Green, P and MacDonald, L W (eds.), *Color Engineering: Achieving Device Independent Colour*, Chichester, UK, John Wiley, 127–164.

Berns, R S and Merrill, R, 2002, 'Color science and painting', *American Artist* January, 68–70, 72.

Berns R S, 2004, 'Rejuvenating Seurat's palette using color and imaging science: a simulation' in Herbert, R L (ed.), *Seurat and the Making of La Grande Jatte*, Art Institute of Chicago and University of California Press, 214–227.

Berns, R S, Byrns, S, Casadio, F, Fiedler, I, Gallagher, C, Imai, F H, Newman, A, Rosen, M R and Taplin, L A, 2004a, 'Rejuvenating the appearance of Seurat's *A Sunday on La Grande Jatte – 1884* using color and imaging science techniques – a simulation' in *Proceedings of the 14th Triennial Meeting The Hague*, ICOM Committee for Conservation.

Berns, R S, Taplin, L A, Imai, F H, Day, E A and Day, D C, 2004b, 'Color accurate image archives using spectral imaging', *Proceedings of the National Academy of Sciences of the United States of America*, in press.

Berns, R S, Taplin, L A, Imai, F H, Day, E A and Day, D C, 2004c, 'A comparison of small-aperture and image-based spectrophotometry of paintings', *Studies in Conservation*, in press.

Fairman, H S, 1997, 'Metameric correction using parametric decomposition', *Color Research and Application* 12, 261–265.

Imai, F H, 1998, 'Multi-spectral image acquisition and spectral reconstruction using a trichromatic digital camera system associated with absorption filters', Munsell Color Science Laboratory Technical Report, http://www.cis.rit.edu/mcsl/research/CameraReports.shtml and available at http://www.art-si.org.

Imai, F H, Berns, R S and Tzeng, D, 2000a 'A comparative analysis of spectral reflectance estimation in various spaces using a trichromatic camera system', *Journal of Imaging Science and Technology* 44, 280–287.

Imai, F H, Rosen, M R and Berns, R S, 2000b, 'Comparison of spectrally narrow-band capture versus wide-band with a priori sample analysis for spectral reflectance estimation' in *Proceedings of the Eighth Color Imaging Conference: Color Science and Engineering, Systems, Technologies and Applications*, Society of Imaging Science and Technology, Springfield, VA , 234–241.

Imai, F H, Taplin, L A and Day, E A, 2002, 'Comparison of the accuracy of various transformations from multi-band images to reflectance spectra', Munsell Color Science Laboratory Technical Report, http://www.art-si.org.

ISO 14524, 1999, 'Photography – Electronic still-picture cameras – Methods for measuring opto-electronic conversion functions (OECFs)', International Organization for Standardization, Geneva, Switzerland.

ISO 17321-1, 2003, 'Graphic technology and photography – Colour characterization of digital still cameras (DSCs) – Part 1: Stimuli, metrology, and test procedures (working draft)', International Organization for Standardization, Geneva Switzerland.

Liang, J, Saunders, D, Cupitt, J and Benchouika, M, 2004, 'A new multi-spectral imaging system for examining paintings' in *Proceedings of the Second European Conference on Color in Graphics, CGIV'2004, Imaging and Vision*, Society of Imaging Science and Technology, Springfield, VA, 229–234.

Mohammadi, M, Nezamabadi, M, Berns, R S and Taplin, L A, 2004, 'Spectral imaging target development based on hierarchical cluster analysis' in *Proceedings of the Twelfth Color Imaging Conference*, Society of Imaging Science and Technology, Springfield, VA, 59–64.

Ribés, A, Brettel, H, Schmitt, F, Liang, H, Cupitt, J and Saunders, D, 2003, 'Color and multispectral imaging with the CRISATEL multispectral system' in *Proceedings PICS Conference*, Society of Imaging Science and Technology, Springfield VA, 215–219.

Saunders, D and Cupitt, J, 1993, 'Image processing at the National Gallery: the VASARI project', *National Gallery Technical Bulletin* 14, 72–85.

Vora, P L and Trussell, H J, 1993, 'Measure of goodness of a set of color scanning filters', *Journal of the Optical Society of America A*,10, 8–23.